

---

# Criticality Leveraged Adversarial Training (CLAT) for Boosted Performance via Parameter Efficiency

---

**Bhavna Gopal<sup>1</sup>, Huanrui Yang<sup>2</sup>, Jingyang Zhang<sup>1</sup>, Mark Horton<sup>1</sup>, Yiran Chen<sup>1</sup>**

<sup>1</sup>Department of Electrical and Computer Engineering, Duke University

<sup>2</sup>Department of Electrical Engineering and Computer Science, University of California, Berkeley

<sup>1</sup>{bhavna.gopal, jingyang.zhang, mark.horton, yiran.chen}@duke.edu, <sup>2</sup>huanrui@berkeley.edu

## Abstract

Adversarial training enhances neural network robustness but suffers from a tendency to overfit and increased generalization errors on clean data. This work introduces CLAT, an innovative approach that mitigates adversarial overfitting by introducing parameter efficiency into the adversarial training process, improving both clean accuracy and adversarial robustness. Instead of tuning the entire model, CLAT identifies and fine-tunes robustness-critical layers—those predominantly learning non-robust features—while freezing the remaining model to enhance robustness. It employs dynamic critical layer selection to adapt to changes in layer criticality throughout the fine-tuning process. Empirically, CLAT can be applied on top of existing adversarial training methods, significantly reduces the number of trainable parameters by approximately 95%, and achieves more than a 2% improvement in adversarial robustness compared to baseline methods.

## 1 Introduction

Advancements in deep learning models have markedly improved image classification accuracy. Despite this, their vulnerability to adversarial attacks — subtle modifications to input images that mislead the model — remains a significant concern [9, 28]. The research community has been rigorously exploring theories to comprehend the mechanics behind adversarial attacks [4]. Ilyas et al. [14] uncover the coexistence of robust and non-robust features in standard datasets. Adversarial vulnerability largely stems from the presence of non-robust features in models trained on standard datasets, which, while highly predictive and beneficial for clean accuracy, are susceptible to noise [28]. Unfortunately, it is observed that deep learning models tend to preferentially learn these non-robust layers. Inkawich et al. [15, 16] further demonstrate that adversarial images derived from the hidden features of certain intermediate non-robust/“critical” layers exhibit enhanced transferability to unseen models. This suggests a commonality in the non-robust features captured by these layers. While identifying these critical layers to improve their robustness is appealing, this process often requires the costly generation of attacks against each individual network layer. Efficient methods to identify and effectively address the criticality of such layers are still lacking.

In contrast to layer-wise feature vulnerability analysis, adversarial training [3, 19, 8], involves training entire neural networks with adversarial examples generated in real-time. This approach inherently encourages all layers in the model to learn robust features from adversarial images, thereby enhancing the model’s resilience against attacks. However, given the more challenging optimization process of learning from adversarial examples than from clean examples, adversarial training also brings hurdles such as heightened errors on clean data and susceptibility to overfitting, ultimately diminishing its effectiveness in practical applications [25, 36, 23, 17]. Despite various efforts to enhance adversarial training, such as modifying input data and adjusting loss functions [12, 23, 36, 30, 32, 21], they still frequently fall short in alleviating the aforementioned challenges.

In light of these challenges, we introduce CLAT, a paradigm shift in adversarial training, where we mitigate overfitting during adversarial training by identifying and tuning only the robustness-critical model layers. CLAT commences by pinpointing critical layers within a model using our novel, theoretically grounded, and easily computable, “**criticality index**”, which we developed to identify layers which have learned non-robust features dominantly. Subsequently, our algorithm meticulously fine-tunes these critical layers to remove their non-robust features and reduce their criticality, while freezing the other, non-critical layers. Dynamic selection of critical layers is conducted during the training process to always focus the fine-tuning on the most-in-need layers, avoiding the overfitting of full-model adversarial training. CLAT therefore enhances both clean and adversarial accuracy compared to previous adversarial training methods. Besides reducing overfitting, the critical layer selection in training also makes CLAT a streamlined, parameter-efficient fine-tuning method, enabling memory savings with its significantly reduced trainable parameters.

In summary, we make the following contributions in this paper:

- We introduce the “criticality index”, a quantitative metric designed to efficiently identify critical layers for the adversarial vulnerability of the model.
- We develop a specialized adversarial training objective focused on reducing the criticality of the identified critical layers to bolster overall model robustness.
- We propose CLAT, a parameter-efficient adversarial fine-tuning algorithm focusing on layer criticality reduction. CLAT mitigates overfitting in the adversarial training process, and applies to various model training scenarios and baseline adversarial training methods.

CLAT stands out by markedly reducing overfitting risks, maintaining or even slightly improving the clean accuracy while significantly enhancing adversarial resilience by at least 2% with a 96% reduction in trainable parameters.

## 2 Related Work

### 2.1 Adversarial training

Adversarial Training (AT) was first introduced by Goodfellow et al. [9], who demonstrated how the integration of adversarial examples into the training process could substantially improve model robustness. This idea evolved into a sophisticated minimax optimization approach with Projected Gradient Descent Adversarial Training (PGD-AT) [19], which employs PGD attacks in training. Regarded as the gold standard in AT, PGD-AT generates adversarial training samples using multiple steps of projected gradient descent, leading to substantially improved empirical robustness [6, 3, 8]. Further refining this approach, TRADES [36] optimizes a novel loss function to balance classification accuracy with adversarial robustness. Recent enhancements in AT, including model ensembling and data augmentation, have also produced notable improvements in model resilience. [33, 34, 7]. Inkawich et al. [15] propose “Activation Attacks” (AA) which underscore the efficacy of leveraging intermediate model layers for generating stronger adversarial attacks, suggesting that incorporating AA in adversarial training could fortify defenses. Their findings provide a foundation for our method which integrates these intermediate critical layers into our adversarial training strategy.

### 2.2 Efficient adversarial training

Adversarial training methods like PGD-AT and TRADES are computationally intensive, necessitating the multi-step generation of adversarial examples, optimization of complex objective functions,

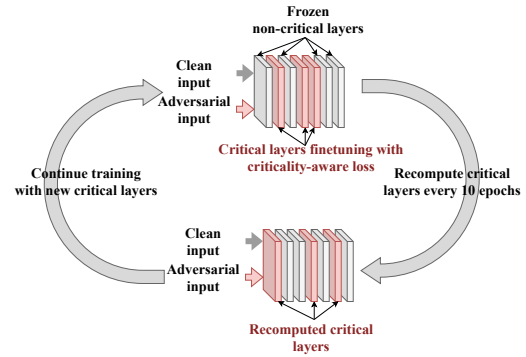


Figure 1: **CLAT overview.** CLAT fine-tunes the selected critical layers (red) while freezing other layers (grey). fine-tuning objective is computed per Equation (9). Critical layers are adjusted periodically. Pseudocode is provided in [Appendix A](#).

and comprehensive model tuning [26]. Numerous efforts to enhance the efficiency of adversarial training have been proposed. Shafahi et al. [26] introduced an efficient model known as ‘‘Free’’ AT, using a single backpropagation step for both training and PGD adversary generation to accelerate adversarial training. However, this approach struggled with maintaining model robustness and increased overfitting, primarily due to gradient alignment issues. Wong et al. [31] then proposed ‘‘Fast’’ AT, which aimed to address these shortcomings, but was later found to be vulnerable to similar problems [2]. As a result, Andriushchenko and Flammarion [2] developed GradAlign but this approach tripled the training time due to second-order gradient computation. Lastly, RiFT leverages network layer redundancies to improve general performance, but its heuristic-based layer redundancy measurement limits final robustness [37]. In contrast, CLAT uses a theoretically grounded, dynamic, critical layer selection mechanism, resulting in a more robust and parameter-efficient adversarial training algorithm. Furthermore, CLAT does not require a fully trained model and can be combined with existing fast-AT methods to enhance performance and mitigate overfitting.

### 3 Methods

Building on prior attack and defense research [15, 16, 37] which demonstrates that not all model layers equally learn non-robust features, we aim to improve model robustness and parameter efficiency by identifying and fine-tuning only those critical layers that are prone to learning non-robust features, while keeping the non-critical layers frozen. In this section, we begin by defining and identifying critical layers, then outline our objectives for reducing their criticality. Finally, we present our complete CLAT algorithm, which effectively enhances model robustness.

#### 3.1 Layer Criticality

Consider a deep learning model with  $n$  layers, and an input  $x$ , defined as:

$$F(x) = f_n(f_{n-1}(\dots f_1(x))), \quad (1)$$

where the functionality of the  $i$ -th layer is denoted as  $f_i$ . During the standard training process, all layers learn useful features which contribute to the correct outputs of the model. We denote the hidden feature learned at the output of the  $i$ -th layer as  $F_i(x) = f_i(f_{i-1}(\dots f_1(x)))$ .

Under adversarial perturbation, features from all layers will be altered, leading to incorrect outputs. To understand how the learned parameters of the model affect the features under perturbation, we consider a function  $G_i(\cdot)$  defined at the output of layer  $i$  on inputs close to a clean data point  $x$ :

$$G_i(z) = \|F_i(z) - F_i(x)\|_2^2. \quad (2)$$

Clearly,  $z = x$  is a minima of  $G_i(z)$ . The worst-case curvature of the function  $G_i$  at the neighborhood of  $z = x$  can be estimated following the formulation by Moosavi-Dezfooli et al. [20] as

$$\nu_i(x) = \frac{\nabla G_i(x') - \nabla G_i(x)}{\|x' - x\|_2} = \frac{\nabla G_i(x')}{\|x' - x\|_2}, \quad (3)$$

where  $x'$  is a worst-case perturbation (adversarial attack) maximizing  $G_i(z)$  in the vicinity of  $x$ , and  $\nabla G_i(x) = 0$  by definition given it is a minimum.

The numerator in the curvature formulation can be further derived as

$$\nu_i(x) = \frac{\frac{\partial F_i(x')}{\partial x'}^T (F_i(x') - F_i(x))}{\|x' - x\|_2}. \quad (4)$$

Following the observation in [20], a higher curvature indicates the feature to be more sensitive to adversarial examples. We can therefore use the curvature formulation  $\nu_i(x)$  under a fixed perturbation budget  $\|x' - x\|_p \leq \epsilon$  to estimate the layer sensitivity, or weakness.

In practice, it is difficult to explicitly instantiate  $\frac{\partial F_i(x')}{\partial x'}$  for a neural network. To this end, we simplify the formulation in Equation (4) by assuming  $\frac{\partial F_i(x')}{\partial x'}$  as a uniform vector. This leads to our definition of the  $\epsilon$ -weakness of layer  $i$ ’s feature as:

$$\mathcal{W}_\epsilon(F_i) = \frac{1}{N_i} \mathbb{E}_x \left[ \sup_{\|\delta\|_p \leq \epsilon} \|F_i(x + \delta) - F_i(x)\|_2 \right], \quad (5)$$

where  $N_i$  denotes the dimensionality of the output features at layer  $i$ , therefore normalizing the weakness measurement of layers with different output sizes. The weakness measurement is proportional to the curvature estimation in Equation (4). A higher weakness value indicates that the feature vector is more vulnerable to input perturbations. The functionality of cascading layers from 1 to  $i$  affects the vulnerability of the hidden features, as described by this formulation.

For the purpose of efficient fine-tuning, we want to identify the layers that are the most critical to the lack of robustness, characterized by their increased susceptibility to perturbations from adversarial inputs. We therefore provide the following definition:

**Definition 3.1. Critical layer:** A layer is considered critical if it exhibits a greater propensity to learn non-robust features or demonstrates heightened sensitivity to adversarial input perturbations relative to other layers in the model.

To this end, we single out the contribution of each layer's functionality to the weakness of the features after it with a *Layer Criticality Index*  $\mathcal{C}_{f_i}$ , which is formulated as

$$\mathcal{C}_{f_i} = \frac{\mathcal{W}_\epsilon(F_i)}{\mathcal{W}_\epsilon(F_{i-1})}. \quad (6)$$

For the first layer, we define  $\mathcal{C}_{f_1} = \mathcal{W}_\epsilon(F_1)$  as only the first layer contributes to the weakness.

As a sanity check, the feature weakness at the output of layer  $i$  can be attributed to the criticality of all previous layers as  $\mathcal{W}_\epsilon(F_i) = \prod_{k=1}^i \mathcal{C}_{f_k}$ . Conversely, a layer with a larger criticality index will increase the weakness of the features after it, indicating the layer is critical according to Definition 3.1, as it heightens the feature sensitivity to the adversarial input.

One drawback of the formulation in Equation (6) is that computing the feature weakness involves finding the worst-case perturbation against the hidden features at each layer, which is a costly process to conduct sequentially for all layers. In practice, we find it possible to approximate the worst-case perturbation against features with an untargeted PGD attack against the model output, so that we can use the same PGD perturbation  $\delta$  to estimate the feature weakness of all layers following Equation (5). In this way, with a reasonably sufficient batch size, we can compute the critical indices for all layers in a model with two forward passes: one with the clean input  $x$  and one with the PGD attack input  $x + \delta$ . We make the following proposition:

**Proposition 3.2.** *Critical layers defined as in Definition 3.1 can be identified as the layers with the largest criticality indices  $\arg \max_i \mathcal{C}_{f_i}$ .*

To verify Proposition 3.2, we conduct an ablation study in Table 5, where we show that model robustness is improved more by CLAT fine-tuning of critical layers compared to equivalent fine-tuning of randomly selected layers. We will discuss how to reduce the criticality of the critical layers and make them more robust in the next subsection.

### 3.2 Criticality-targeted fine-tuning

Once the critical layers are identified, we fine-tune them to reduce their criticality, thereby decreasing the weakness of subsequent hidden features and enhancing model robustness. For a critical layer  $i$ , we optimize the trainable parameters to minimize  $\mathcal{C}_{f_i}$ . Note that in the criticality formulation in Equation (6), the weakness of the previous layer's output,  $\mathcal{W}_\epsilon(F_{i-1})$ , is constant with respect to  $f_i$ . Thus, the optimization objective for  $f_i$  can be simplified as

$$\mathcal{L}_C(f_i) = \mathbb{E}_x \left[ \sup_{\|\delta\|_p \leq \epsilon} \|F_i(x + \delta) - F_i(x)\|_2 \right]. \quad (7)$$

In the case where multiple critical layers are considered in the fine-tuning process, the fine-tuning objective can be expanded to accommodate all critical layers simultaneously. Formally, suppose we have a set  $S$  where layers  $i \in S$  are all selected for fine-tuning, the fine-tuning objective for these critical layers can be formulated as

$$\mathcal{L}_C(f_S) = \mathbb{E}_x \left[ \sup_{\|\delta\|_p \leq \epsilon} \sum_{i \in S} \|F_i(x + \delta) - F_i(x)\|_2 \right], \quad (8)$$

where a single perturbation is utilized to capture the weakness across all critical layers. In practice, a projected gradient ascent optimization with random start is used to solve the inner maximization.

Minimizing the objective in Equation (8) by adjusting the trainable variables of the critical layers will reduce their feature weaknesses. However, the removal of non-robust features in these layers may affect the functionality of the model on clean inputs. As a tradeoff, we also include the cross entropy loss  $\mathcal{L}(\cdot)$  in the final optimization objective, which derives the optimization objective on the critical layers during the fine-tuning process

$$\min_{f_S} \mathbb{E}_{x,y} \mathcal{L}(F(x), y) + \lambda \mathcal{L}_C(f_S), \quad (9)$$

where the hyperparameter  $\lambda$  serves as a balancing factor between the two loss terms. Note that only the selected critical layers  $f_S$  are optimized in Equation (9) while the other non-critical layers are frozen, justifying our fine-tuning to be parameter-efficient.

### 3.3 CLAT adversarial training

Similar to parameter-efficient fine-tuning techniques in other domains, we design CLAT as a fine-tuning approach, which is applied to neural networks that have undergone preliminary training. The pretraining phase allows all layers in the model to capture useful features, which will facilitate the identification of critical layers in the model. Notably, CLAT’s versatility allows it to adapt to various types of pretrained models, either adversarially trained or trained on a clean dataset only. In practice, we find that models do not need to fully converge during the pretraining phase to benefit from CLAT fine-tuning. For example, in case of the CIFAR-10 dataset, 50 epochs of PGD-AT training would be adequate. We consider the number of adversarial pretraining epochs as a hyperparameter and provide further analysis on the impact of pretraining epochs in Section 4.3.1.

After the pretraining, CLAT begins by identifying and selecting critical layers in the pretrained model. We then fine-tune critical layers only while freezing the rest of the layers. This process is illustrated in Figure 1, and the pseudocode is provided in Algorithm 1 in **Appendix A** for greater clarity. Compared to full-model fine-tuning, CLAT not only improves parameter efficiency with fewer trainable parameters, but also reduces overfitting, a common issue in standard adversarial training. As fine-tuning progresses, the critical layers will be updated to reduce their criticality, making them less critical than some of the previously frozen layers. Subsequently, we perform periodic reevaluation of the top  $k$  critical indices, ensuring continuous adaptation and optimization of the layers that are the most in need in the training process. Through hyperparameter optimization, we find 10 epochs to be adequate to optimize the selected critical layers for all models that we tested.

## 4 Experiments

### 4.1 Experimental settings

**Datasets and models** We conducted experiments using two widely recognized image classification datasets, CIFAR10 and CIFAR100. Each dataset includes 60,000 color images, each  $32 \times 32$  pixels, divided into 10 and 100 classes respectively [18]. For our experiments, we deployed a suite of network architectures: WideResnets (34-10, 70-16) [35], ResNets (50, 18) [11], DenseNet-121 [13], PreAct ResNet-18[10], and VGG-19 [27]. In this paper, these architectures are referred to as WRN34-10, WRN70-16, RN50, RN18, DN121, Preact RN18 and VGG19 respectively.

**Training and evaluation** Since CLAT can be layered over clean pretraining, partial training, or other adversarial methods, results incorporating CLAT are denoted in our tables as "X+ CLAT," where "X" specifies the baseline method used prior to applying CLAT. Typically, this baseline method was applied for the first 50 epochs, followed by a fine-tuning phase during which CLAT was run for an additional 50 epochs. Models trained exclusively with PGD-AT typically require 150 epochs to achieve reported performances. We use PGD for attack generation unless stated otherwise in the baseline method, which employs a random start [19], with an attack budget of  $\epsilon = 0.03$  under the  $\ell_\infty$  norm, an update step size of  $\alpha = 0.007$ , and 10 attack steps. Experiments were conducted on a Titan XP GPU, starting with an initial learning rate of 0.1, which was adjusted according to a cosine decay schedule. To ensure the reliability of robustness measurements, we conducted each experiment a minimum of 10 times, reporting the lowest adversarial accuracies we observed.

**CLAT settings** We select critical layers as described in Section 3.1. Table 3 outlines the Top-5 most critical layers for some of the models and corresponding datasets at the start of the CLAT fine-tuning, after adversarially training with PGD-AT for 50 epochs. In customizing the CLAT methodology to various network sizes, we select approximately 5% of layers as critical through hyperparameter optimization. For instance, DN121 uses 5 critical layers, while WRN70-16, RN50, WRN34-10, VGG19, and RN18 use 4, 3, 2, 1, and 1 critical layers, respectively.

## 4.2 CLAT performance

**White-box robustness** Table 1 presents the clean accuracy and white-box  $\ell_\infty$  PGD [6] accuracy across various adversarial training techniques. The versatility and effectiveness of CLAT are demonstrated by combining it with various standard adversarial training methods. CLAT mitigates the overfitting commonly observed in traditional adversarial training methods, improving both clean and adversarial accuracy compared to the corresponding baselines.

We also show that reducing trainable parameters alone does not guarantee a performance improvement by comparing CLAT against other parameter-efficient fine-tuning methods like LoRA [1] and RiFT [37]. Our theoretically-grounded criticality indices enable the precise identification of critical layers and the focused elimination of non-robust features from these pivotal layers. Furthermore, we verify that fast adversarial training techniques as in [31] can be applied to solve the inner maximization in the CLAT training objective in Equation (8), where the ‘‘CLAT (Fast)’’ method also improves performance and robustness over Fast-AT baselines.

Besides the main table, we provide additional robustness results in **Appendix B**, where we showcase CLAT’s improved robustness against a variant of the white-box Auto Attack [8] in Table 8 and verify the generalizability of the robustness to attacks of various strengths in Figure 4.

**Black-box robustness** Table 2 evaluates the robustness against black-box attacks between models trained solely using PGD-AT and those augmented with CLAT. Attack settings are the same as those of the white-box attacks. As a sanity check, the accuracies under black-box attack surpass those observed under white-box scenarios, indicating that gradient masking does not appear in the CLAT model, and that the white-box robustness evaluation is valid. More significantly, models trained with CLAT consistently outperform those trained with PGD-AT, maintaining superior resilience in both black-box and white-box settings, regardless of the attack method or models employed.

## 4.3 Ablation Studies

### 4.3.1 Ablating on pretraining epochs before CLAT

As discussed in Section 3.3, we apply CLAT after the model has been adversarially trained for some epochs. Here, we analyze how the number of pretraining epochs affects CLAT performance. Figure 2 shows the training curves for different allocations of PGD pretraining epochs and CLAT fine-tuning epochs within a 100-epoch training budget. The overfitting of PGD-AT is evident as adversarial accuracy plateaus and declines towards the end, as documented in previous research [24]. In contrast, CLAT continues to improve adversarial accuracy, effectively addressing this issue. Including CLAT at any stage of training results in higher clean accuracy and robustness at convergence. Additional results on pretrained clean models are provided in **Appendix C**.

Furthermore, an intriguing aspect of our experiments involves running CLAT from scratch (0 PGD-AT epochs). Although CLAT ultimately surpasses PGD-AT with sufficient epochs, using CLAT without any prior adversarial training results in significantly slower model convergence. We believe this suggests that ‘‘layer criticality’’ emerges during the adversarial training process, allowing critical layers to be identified as the model undergoes adversarial training. This phenomenon supports our theoretical insight that criticality can be linked to the curvature of the local minima to which each layer converges during adversarial training. Flattening the local minima of critical layers aids in model generalization. We plan to explore this phenomenon further in future work.

### 4.3.2 Ablating on critical layer selection

The choice of critical layer selection is another important feature impacting the performance of CLAT. We begin by examining the effect of dynamic layer selection. Table 4 highlights that dynamic

Table 1: Comparative performance of CLAT across various networks and adversarial training/fine-tuning techniques. Robustness is evaluated with white-box PGD attacks.

MODEL	METHOD	CIFAR-10 ACC. (%)		CIFAR-100 ACC. (%)	
		CLEAN	ADVERSARIAL	CLEAN	ADVERSARIAL
DN121	PGD-AT [19]	80.05	58.15	57.18	31.76
	<b>PGD-AT + CLAT</b>	<b>81.03</b>	<b>60.60</b>	<b>58.79</b>	<b>33.23</b>
WRN70-16	PENG ET AL. [22]	93.27	71.07	70.20	42.61
	<b>PENG ET AL. + CLAT</b>	<b>93.56</b>	<b>72.25</b>	<b>71.94</b>	<b>44.12</b>
	BAI ET AL. [5]	92.23	64.55	69.17	40.86
	<b>BAI ET AL. + CLAT</b>	<b>92.77</b>	<b>64.92</b>	<b>70.17</b>	<b>41.64</b>
RN50	PGD-AT	81.38	56.35	58.16	33.01
	<b>PGD-AT + CLAT</b>	<b>83.78</b>	<b>59.54</b>	<b>61.88</b>	<b>36.23</b>
WRN34-10	PGD-AT	87.41	55.40	59.19	31.66
	PGD-AT + LORA [1]	73.36	56.17	55.56	31.43
	PGD-AT + RIFT [37]	87.89	55.41	62.35	31.64
	<b>PGD-AT + CLAT</b>	<b>88.97</b>	<b>57.11</b>	<b>62.38</b>	<b>32.05</b>
	TRADES [36]	87.60	56.61	60.56	31.85
	TRADES + RIFT	87.55	56.72	61.01	32.03
	<b>TRADES + CLAT</b>	<b>88.23</b>	<b>57.89</b>	<b>61.45</b>	<b>33.56</b>
VGG19	PGD-AT	78.38	50.35	50.16	26.54
	<b>PGD-AT + CLAT</b>	<b>79.88</b>	<b>52.54</b>	<b>50.98</b>	<b>28.41</b>
RN18	PGD-AT	81.46	53.63	57.10	30.15
	PGD-AT + LORA	76.57	55.38	48.49	32.36
	PGD-AT + RIFT	83.44	53.65	58.74	30.17
	<b>PGD-AT + CLAT</b>	<b>83.89</b>	<b>55.37</b>	<b>59.22</b>	<b>32.04</b>
	TRADES	81.54	53.31	57.44	30.20
	TRADES + RIFT	81.87	53.30	57.78	30.22
	<b>TRADES + CLAT</b>	<b>81.89</b>	<b>54.57</b>	<b>58.82</b>	<b>31.06</b>
	MART [29]	76.77	56.90	51.46	31.47
	MART + RIFT	77.14	56.92	52.42	31.48
	<b>MART + CLAT</b>	<b>76.82</b>	<b>57.55</b>	<b>53.01</b>	<b>33.23</b>
	AWP [32]	78.40	53.83	52.85	31.00
	AWP + RIFT	78.79	53.84	54.89	31.05
	<b>AWP + CLAT</b>	<b>79.01</b>	<b>55.27</b>	<b>55.39</b>	<b>32.08</b>
	SCORE [21]	84.20	54.59	54.83	29.49
	SCORE + RIFT	85.65	54.62	57.63	29.50
	<b>SCORE + CLAT</b>	<b>86.11</b>	<b>55.78</b>	<b>57.66</b>	<b>30.23</b>
PREACT RN18	FAST-AT [31]	81.46	45.55	50.10	27.72
	<b>FAST-AT + CLAT</b>	<b>84.46</b>	<b>52.13</b>	<b>54.33</b>	<b>29.22</b>
	<b>FAST-AT + CLAT (FAST)</b>	<b>82.72</b>	<b>49.62</b>	<b>52.10</b>	<b>27.99</b>

selection is crucial to CLAT’s performance. Using the same layers throughout the process tends to cause overfitting and results in lower accuracies compared to the PGD-AT baseline.

To verify the significance of the selected critical layers, we compare CLAT with an alternative approach in which random layers are dynamically selected for fine-tuning instead of the critical layers. The results of this comparison are detailed in Table 5 and Table 10 (in **Appendix C**) on CIFAR-10 and CIFAR-100, respectively. The data demonstrates that selecting critical layers significantly enhances the model’s adversarial robustness and yields a marginal increase in clean accuracy. Moreover, Table 3 indicates near-identical critical layer selections within the same model even across diverse datasets. This evidence supports our assertion that the variation in layer criticality stems from inherent properties within the model architecture, wherein certain layers are predisposed to learning non-robust features.

Lastly, we ablate on the number of critical layers used in CLAT for fine-tuning. Figure 3 illustrates the trade-off between adversarial test accuracy and the quantity of critical layers selected for fine-tuning. Allowing more layers to be fine-tuned enhances the model flexibility, which initially improves CLAT performance. However, fine-tuning an excessive proportion of critical layers diminishes CLAT’s effectiveness. This is likely due to the diversion of attention towards fine-tuning less-critical layers,

Table 2: Comparative Analysis of Black-box PGD Accuracy on CIFAR-10 and CIFAR100. Model in each row is the attacker and each column the victim.

NETWORK	METHOD	CIFAR-10 ADV. ACC. (%)				CIFAR-100 ADV. ACC. (%)			
		RN50	DN121	VGG19	RN18	RN50	DN121	VGG19	RN18
RN50	PGD-AT	-	74.83	68.01	67.44	-	46.82	40.55	40.10
	CLAT	-	76.45	71.25	70.12	-	48.49	44.34	43.91
DN121	PGD-AT	72.24	-	69.53	68.38	44.45	-	40.63	41.22
	CLAT	74.55	-	71.78	70.56	46.78	-	43.62	42.88
VGG19	PGD-AT	65.72	67.56	-	62.26	47.86	46.56	-	40.55
	CLAT	66.46	70.72	-	65.78	49.25	48.72	-	42.72
RN18	PGD-AT	74.82	70.21	61.83	-	46.28	45.59	39.21	-
	CLAT	76.23	73.19	63.96	-	48.89	47.72	41.78	-

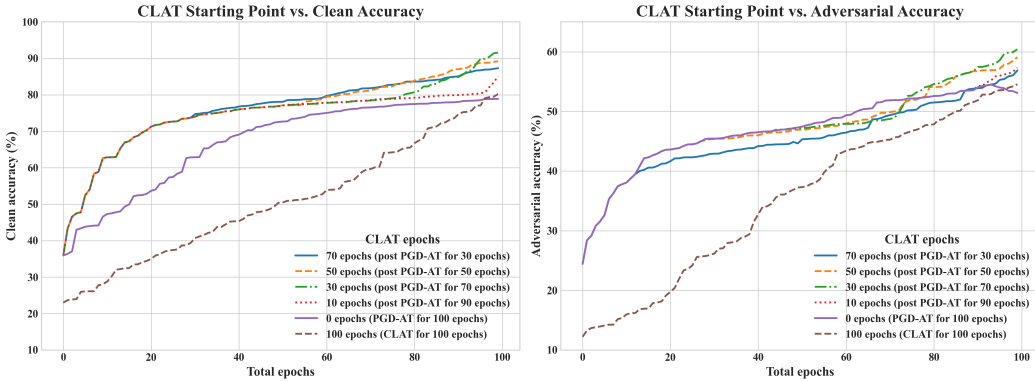


Figure 2: Comparative analysis of CLAT performance on WRN34-10: Clean and adversarial accuracy on CIFAR-10 across partially trained models. Note: PGD-AT requires 150 epochs to fully converge.

detracting from more critical ones. This pattern highlights the crucial influence of specific layers on network robustness and suggests a need for deeper research to understand the roles and dynamics of individual layers influencing network robustness.

#### 4.4 Efficiency and stability analysis

To verify the significance of the selected critical layers, we contrast CLAT with an alternative approach in which random layers are dynamically selected for fine-tuning instead of the critical layers. The

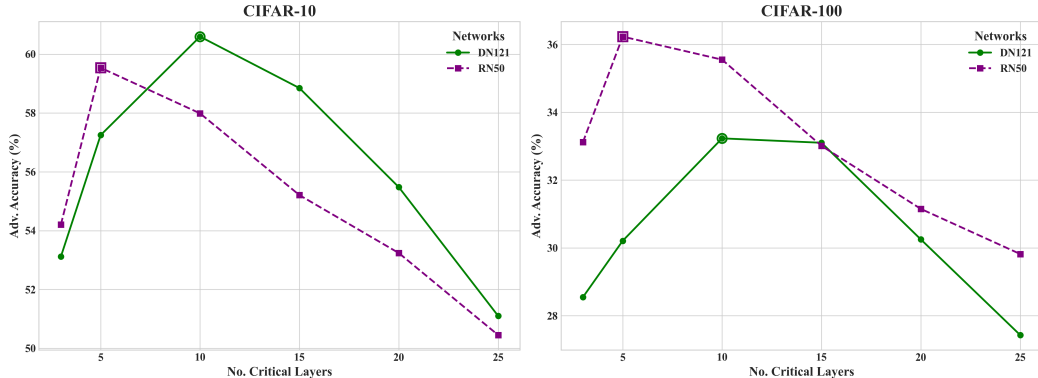


Figure 3: Comparative analysis on CLAT performance/adversarial accuracy with respect to number of critical layers used during CLAT

Table 3: Top-5 criticality indices by model and dataset. Layers used in CLAT are bolded.

MODEL	CIFAR10	CIFAR100
DN121	<b>39, 14, 1, 3, 88</b>	<b>39, 15, 1, 2, 91</b>
WRN70-16	<b>4, 17, 1, 59, 62</b>	<b>3, 17, 2, 59, 61</b>
RN50	<b>34, 41, 48, 3, 36</b>	<b>34, 43, 45, 6, 32</b>
WRN34-10	<b>26, 1</b> 30, 3, 28	<b>26, 2</b> , 30, 3, 27
VGG19	<b>9, 11, 5, 3, 1</b>	<b>8, 13, 5, 3, 1</b>
RN18	<b>11, 10, 4, 2, 12</b>	<b>12, 9, 5, 2, 13</b>

Table 5: Critical vs. random layers for CLAT on CIFAR-10.

NETWORK	CIFAR-10			
	CRITICAL LAYERS		RANDOM LAYERS	
CLEAN ACC.	ADV. ACC.	CLEAN ACC.	ADV. ACC.	
DN121	81.03	60.60	78.85	51.35
RN50	83.78	59.54	79.01	51.44
RN18	83.89	55.37	78.02	51.03

results of this comparison are detailed in Table 5 and Table 10 (in **Appendix C**) on CIFAR-10 and CIFAR-100, respectively.

The cost of optimizing the CLAT training objective in Equation (9) is similar to that of the standard adversarial training given its min-max formulation. Here, we show that the computational overhead for determining critical indices is negligible. We verify in Table 7 that criticality indices can be stably computed with a single training batch as small as 10, with top-ranking layers consistent with those achieved with a larger batch. We further conducted over 1000 runs for each network to randomly select the data used for criticality estimation, where we find remarkable consistency in computed critical layers, differing in less than 5% of cases, typically involving only one layer change among the top five critical layers. The stability means we can use a mere 0.0002% of the training data for criticality estimation every 10 epochs, which introduces neglectable additional complexity to the training process as indicated by the time measurement in the table.

Table 7: DenseNet-121 critical layers identified with different amount of data. Time taken to compute critical layers evaluated on TITAN RTX GPU. As a reference, 1 PGD-AT epoch takes 67s.

BATCH SIZE	CIFAR10		CIFAR100	
	CRITICAL LAYERS	TIME (S)	CRITICAL LAYERS	TIME(S)
10	39, 14, 1, 3, 90	2.64	39, 15, 1, 2, 91	2.82
30	39, 14, 1, 3, 88	2.72	39, 15, 1, 2, 88	2.91
50	39, 14, 1, 3, 89	2.83	39, 15, 1, 3, 91	3.14
100	39, 14, 1, 3, 88	3.15	39, 15, 1, 2, 91	3.54

## 5 Conclusions

In this work, we introduce CLAT, an innovative adversarial training approach that addresses adversarial overfitting issues by fine-tuning only the critical layers vulnerable to adversarial perturbations. This method not only emphasizes layer-specific interventions for enhanced network robustness but also sheds light on the commonality in non-robust features captured by these layers, offering a targeted and effective defense strategy. Our results reveal that CLAT reduces trainable parameters by about 95% while ensuring significant improvements in clean accuracy and adversarial robustness across diverse network architectures and baseline adversarial training methods. We limit the scope of this work to improving the empirical robustness of the model by utilizing the critical layers. In this sense, open questions remain on why these specific layers become critical, whether they can be identified more effectively, and whether the issues can be resolved with architectural or training scheme changes. We leave a more theoretical understanding of these questions as future work.

Table 4: Comparison of PGD-AT, PGD-AT + CLAT, and PGD-AT + CLAT (Non-dynamic) on CIFAR-10 Adv. Accuracy.

METHOD	DN121	RN50
PGD-AT	58.15	56.35
CLAT	60.60	59.54
CLAT (ND)	57.01	54.22

Table 6: Trainable Parameters during CLAT in Various Networks

NETWORK	TRAINABLE PARAMS		% USED
	TOTAL	CLAT	
DN121	6.96M	217K	3.1%
WRN70-16	267M	8.29M	3.0%
RN50	23.7M	823K	3.4%
WRN34-10	46.16M	1.24M	2.7%
RN18	11.2M	590K	5.2%
VGG19	39.3M	236K	6.0%

## References

- [1] Sidra Aleem, Julia Dietlmeier, Eric Arazo, and Suzanne Little. Convlora and adabn based domain adaptation via self-training. *arXiv preprint arXiv:2402.04964*, 2024.
- [2] Maksym Andriushchenko and Nicolas Flammarion. Understanding and improving fast adversarial training, 2020.
- [3] Anish Athalye, Nicholas Carlini, and David Wagner. Obfuscated gradients give a false sense of security: Circumventing defenses to adversarial examples, 2018.
- [4] Tao Bai, Jinqi Luo, Jun Zhao, Bihan Wen, and Qian Wang. Recent advances in adversarial training for adversarial robustness, 2021.
- [5] Yatong Bai, Brendon G. Anderson, Aerin Kim, and Somayeh Sojoudi. Improving the accuracy-robustness trade-off of classifiers via adaptive smoothing, 2024.
- [6] Nicholas Carlini and David Wagner. Towards evaluating the robustness of neural networks, 2017.
- [7] Yair Carmon, Aditi Raghunathan, Ludwig Schmidt, Percy Liang, and John C. Duchi. Unlabeled data improves adversarial robustness, 2022.
- [8] Francesco Croce and Matthias Hein. Reliable evaluation of adversarial robustness with an ensemble of diverse parameter-free attacks, 2020.
- [9] Ian J. Goodfellow, Jonathon Shlens, and Christian Szegedy. Explaining and harnessing adversarial examples, 2015.
- [10] Kaiming He, Xiangyu Zhang, Shaoqing Ren, and Jian Sun. Identity mappings in deep residual networks, 2016.
- [11] Kaiming He, Xiangyu Zhang, Shaoqing Ren, and Jian Sun. Deep residual learning for image recognition. In *Proceedings of the IEEE conference on computer vision and pattern recognition*, pages 770–778, 2016.
- [12] Dorjan Hitaj, Giulio Pagnotta, Iacopo Masi, and Luigi V. Mancini. Evaluating the robustness of geometry-aware instance-reweighted adversarial training, 2021.
- [13] Gao Huang, Zhuang Liu, Laurens Van Der Maaten, and Kilian Q Weinberger. Densely connected convolutional networks. In *Proceedings of the IEEE conference on computer vision and pattern recognition*, pages 4700–4708, 2017.
- [14] Andrew Ilyas, Shibani Santurkar, Dimitris Tsipras, Logan Engstrom, Brandon Tran, and Aleksander Madry. Adversarial examples are not bugs, they are features. *Advances in neural information processing systems*, 32, 2019.
- [15] Nathan Inkawich, Wei Wen, Hai (Helen) Li, and Yiran Chen. Feature space perturbations yield more transferable adversarial examples. In *Proceedings of the IEEE/CVF Conference on Computer Vision and Pattern Recognition (CVPR)*, June 2019.
- [16] Nathan Inkawich, Kevin Liang, Binghui Wang, Matthew Inkawich, Lawrence Carin, and Yiran Chen. Perturbing across the feature hierarchy to improve standard and strict blackbox attack transferability. *Advances in Neural Information Processing Systems*, 33:20791–20801, 2020.
- [17] Adel Javanmard, Mahdi Soltanolkotabi, and Hamed Hassani. Precise tradeoffs in adversarial training for linear regression, 2020.
- [18] Alex Krizhevsky and Geoffrey Hinton. Learning multiple layers of features from tiny images. 2009.
- [19] Aleksander Madry, Aleksandar Makelov, Ludwig Schmidt, Dimitris Tsipras, and Adrian Vladu. Towards deep learning models resistant to adversarial attacks, 2019.

[20] Seyed-Mohsen Moosavi-Dezfooli, Alhussein Fawzi, Jonathan Uesato, and Pascal Frossard. Robustness via curvature regularization, and vice versa. In *Proceedings of the IEEE/CVF Conference on Computer Vision and Pattern Recognition*, pages 9078–9086, 2019.

[21] Tianyu Pang, Min Lin, Xiao Yang, Jun Zhu, and Shuicheng Yan. Robustness and accuracy could be reconcilable by (proper) definition, 2022.

[22] ShengYun Peng, Weilin Xu, Cory Cornelius, Matthew Hull, Kevin Li, Rahul Duggal, Mansi Phute, Jason Martin, and Duen Horng Chau. Robust principles: Architectural design principles for adversarially robust cnns, 2023.

[23] Aditi Raghunathan, Sang Michael Xie, Fanny Yang, John C Duchi, and Percy Liang. Adversarial training can hurt generalization. *arXiv preprint arXiv:1906.06032*, 2019.

[24] Leslie Rice, Eric Wong, and J. Zico Kolter. Overfitting in adversarially robust deep learning, 2020.

[25] Ludwig Schmidt, Shibani Santurkar, Dimitris Tsipras, Kunal Talwar, and Aleksander Madry. Adversarially robust generalization requires more data, 2018.

[26] Ali Shafahi, Mahyar Najibi, Amin Ghiasi, Zheng Xu, John Dickerson, Christoph Studer, Larry S. Davis, Gavin Taylor, and Tom Goldstein. Adversarial training for free!, 2019.

[27] Karen Simonyan and Andrew Zisserman. Very deep convolutional networks for large-scale image recognition. In *3rd International Conference on Learning Representations, ICLR 2015 - Conference Track Proceedings*, 2015.

[28] Christian Szegedy, Wojciech Zaremba, Ilya Sutskever, Joan Bruna, Dumitru Erhan, Ian Goodfellow, and Rob Fergus. Intriguing properties of neural networks, 2014.

[29] Yisen Wang, Difan Zou, Jinfeng Yi, James Bailey, Xingjun Ma, and Quanquan Gu. Improving adversarial robustness requires revisiting misclassified examples. In *International conference on learning representations*, 2019.

[30] Yisen Wang, Difan Zou, Jinfeng Yi, James Bailey, Xingjun Ma, and Quanquan Gu. Improving adversarial robustness requires revisiting misclassified examples. In *International Conference on Learning Representations*, 2020. URL <https://openreview.net/forum?id=rk10g6EFwS>.

[31] Eric Wong, Leslie Rice, and J. Zico Kolter. Fast is better than free: Revisiting adversarial training, 2020.

[32] Dongxian Wu, Shu tao Xia, and Yisen Wang. Adversarial weight perturbation helps robust generalization, 2020.

[33] Cihang Xie, Mingxing Tan, Boqing Gong, Jiang Wang, Alan Yuille, and Quoc V. Le. Adversarial examples improve image recognition, 2020.

[34] Huanrui Yang, Jingyang Zhang, Hongliang Dong, Nathan Inkawich, Andrew Gardner, Andrew Touchet, Wesley Wilkes, Heath Berry, and Hai Li. Dverge: diversifying vulnerabilities for enhanced robust generation of ensembles. *Advances in Neural Information Processing Systems*, 33:5505–5515, 2020.

[35] Sergey Zagoruyko and Nikos Komodakis. Wide residual networks, 2017.

[36] Hongyang Zhang, Yaodong Yu, Jiantao Jiao, Eric P. Xing, Laurent El Ghaoui, and Michael I. Jordan. Theoretically principled trade-off between robustness and accuracy, 2019.

[37] Kaijie Zhu, Jindong Wang, Xixu Hu, Xing Xie, and Ge Yang. Improving generalization of adversarial training via robust critical fine-tuning, 2023.

## A Pseudocode of CLAT

To better facilitate an understanding of the CLAT process, we illustrate the pseudocode of the dynamic critical layer identification process and the criticality-targeted fine-tuning process in **Algorithm 1**. Only the selected critical layers are being fine-tuned while all the other layers are frozen.

---

### Algorithm 1 CLAT Algorithm

---

```

1: Input: Dataset  $\mathcal{D}$ , pre-trained model  $F$ , batch size  $bs$ , total epochs  $N$ .
2: for  $epoch = 1$  to  $N$  do
3:   if  $epoch \% 10 == 1$  then
4:     # Find critical layers
5:      $x \leftarrow$  Batch of training data in  $\mathcal{D}$ 
6:      $x + \delta \leftarrow$  PGD attack against  $F$ 
7:     Compute  $\mathcal{W}_\epsilon(F_i)$  for all layers with Equation (5)
8:     Compute  $\mathcal{C}_{f_i}$  for all layers with Equation (6)
9:     Critical layers  $\mathcal{S} \leftarrow TopK(\mathcal{C}_{f_i})$ 
10:    # fine-tune critical layers
11:     $minibatches \leftarrow CreateMinibatches(\mathcal{D}, bs)$ 
12:    for  $x, y$  in  $minibatches$  do
13:      Perturbation  $\delta \leftarrow$  Equation (8) inner maximization
14:       $\mathcal{L}_C(f_{\mathcal{S}}) \leftarrow$  Equation (8)
15:      Weight update  $w[\mathcal{S}]$  with Equation (9)

```

---

## B Additional experiment results

Table 8 showcases results under a variant of the white-box Auto Attack [8] with an epsilon value of 0.03 and a single restart in Table 1. Specifically, we report adversarial accuracies of the “APGD<sub>CE</sub>” untargeted attack, a component of the Auto Attack ensemble, with similar trends observed for other attacks in the ensemble.

Although CLAT models employ PGD-like attacks on hidden features during the adversarial training phase and have not seen Auto Attacks, the robustness remains under Auto Attacks. This highlights the similarity in non-robust features utilized by different attacks in different networks. As CLAT resolves the non-robust features with critical layer fine-tuning, the resulting robustness is generalizable across attack settings and source models of the attacks.

Table 8: Adversarial accuracy under the white-box “APGD<sub>CE</sub>” variant of Auto Attack: Models trained using CLAT consistently outperform those trained exclusively with PGD-AT.

DATASET	NETWORK	PGD-AT(%)	PGD-AT + CLAT (%)
CIFAR-10	DN121	49.26	<b>50.58</b>
	WRN70-16	54.48	<b>56.90</b>
	RN50	48.54	<b>50.65</b>
	WRN34-10	52.21	<b>54.73</b>
	VGG19	45.35	<b>47.01</b>
	RN18	46.99	<b>48.20</b>
CIFAR-100	DN121	24.67	<b>26.31</b>
	WRN70-16	30.27	<b>33.32</b>
	RN50	25.44	<b>26.64</b>
	WRN34-10	27.62	<b>31.53</b>
	VGG19	22.50	<b>24.02</b>
	RN18	23.81	<b>24.43</b>

We further compare the CLAT model robustness with the robustness of the SAT model against white-box attacks of various strengths. As illustrated in Figure 4, though both models are only

trained against an attack of one strength ( $\epsilon = 0.03$ ), the improved robustness of CLAT is consistent across the full spectrum of attack strengths. This shows that CLAT is not overfitting to the specific attack strength used in training.

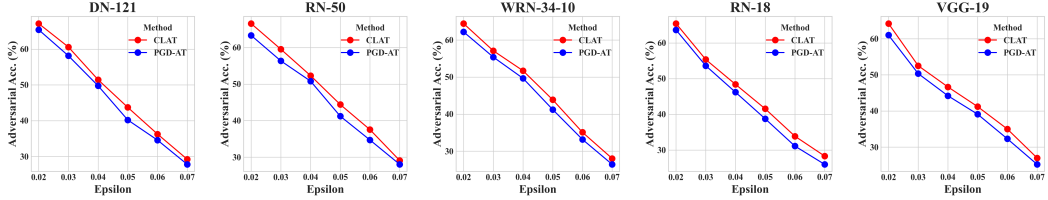


Figure 4: White-box adversarial accuracy (y-axis) on CIFAR-10 for models trained with CLAT (red) and PGD-AT (blue), against PGD attacks of varying strengths (x-axis)

## C Additional ablation study

### C.1 CLAT on pretrained clean model

Besides the discussion on performing CLAT after adversarial pretraining in Section 4.3.1, Table 9 details the performance of CLAT on clean pretrained models. Although the adversarial accuracies of clean pretrained models are relatively low compared to those of adversarially trained models, CLAT demonstrates its capability to facilitate adversarial fine-tuning on clean models effectively to some extent. This is a novel achievement, showcasing the algorithm’s versatility.

Table 9: Adversarial and clean accuracies for performing CLAT on various PyTorch pretrained models on the CIFAR-10 dataset.

MODEL	ADV. ACC.	CLEAN ACC.
DN-121	39.21%	80.89%
WRN70-16	42.1%	83.35%
RN-50	35.67%	78.23%
WRN34-10	40.1%	81.78%
VGG-19	32.67%	75.05%
RN-18	34.45%	76.51%

### C.2 Additional results on layer selection

Here in Table 10, we provide additional results contrasting CLAT with an alternative approach where random layers are dynamically selected for fine-tuning instead of the critical layers on the CIFAR-100 dataset.

Table 10: Ablating the layer choices for CLAT fine-tuning on CIFAR-100.

NETWORK	CIFAR-100			
	CRITICAL LAYERS		RANDOM LAYERS	
	CLEAN ACC.	ADV. ACC.	CLEAN ACC.	ADV. ACC.
DN121	58.79	33.23	54.85	23.32
RN50	61.88	36.23	56.50	22.45
RN18	59.22	32.04	52.43	22.60